Separation Science and Technology
Publication details, including instructions for authors and subscription information:
http://www.informaworld.com/smpp/title~content=t713708471

Gas Separation in a Membrane Unit: Experimental Results and Theoretical Predictions

L. Tranchino[ab]; R. Santarossa[a]; F. Carta[a]; C. Fabiani[c]; L. Bimbi[c]
[a] ENIRICERCHE S.p.A., MONTEROTONDO, ROME, ITALY [b] CTB, via Sardegna 38, Rome, Italy [c] ENEA, TIB-CHEMICAL DIVISION CRE-CASACCIA, ROME, ITALY

To cite this Article Tranchino, L. , Santarossa, R. , Carta, F. , Fabiani, C. and Bimbi, L.(1989) 'Gas Separation in a Membrane Unit: Experimental Results and Theoretical Predictions', Separation Science and Technology, 24: 14, 1207 — 1226
To link to this Article: DOI: 10.1080/01496398908049898
URL: http://dx.doi.org/10.1080/01496398908049898

SEPARATION SCIENCE AND TECHNOLOGY, 24(14), pp. 1207-1226, 1989

Gas Separation in a Membrane Unit: Experimental Results and Theoretical Predictions

L. TRANCHINO,* R. SANTAROSSA, and F. CARTA

ENIRICERCHE S.p.A.
00015 MONTEROTONDO, ROME, ITALY

C. FABIANI and L. BIMBI

ENEA, TIB-CHEMICAL DIVISION
CRE-CASACCIA, ROME, ITALY

Abstract

A laboratory membrane separation unit was assembled by using composite hollow fibers. It was tested in an automated apparatus for gas separation measurements. The performances of the system were measured for CH_4/CO_2 mixtures as functions of temperature, pressure, stage cut, feed gas composition, and flow regime. The results were analyzed on the basis of a predictive mathematical model of the process. A good fitting of the data was obtained in most cases except at high pressure, probably as a consequence of structural changes of the active layer of the fibers under pressurization.

1. INTRODUCTION

In the last few years, remarkable progress has been made in the field of membrane separation technology, particularly for gas purification (*1-3*).

Improvements in such processes derive mainly from a deeper understanding of the relationships between membrane structure and properties and the consequent possibility of preparing new highly selective and

*Present address: CTB, via Sardegna 38, 00187 Rome, Italy.

permeable membranes, although, for many gaseous mixtures, membranes are in general not very selective. But improvements can also derive from progress in the process engineering of these new unit operations designed to take maximum advantage of the potential of membrane properties.

It is worth noting that the extent of separation achieved in a membrane process is not a function of the membrane characteristics only; it can be considerably enhanced by process design techniques: appropriate selection of operative conditions, flow regimes, etc., or application of new concepts such as the use of a recycle permeator, a continuous membrane column, multimembrane permeators, etc. (*1*, *2*).

In the present work, process engineering aspects of membrane separation are taken into account to study the behavior of a gas separation module and to show possible departures from a simple theoretical model of the transport phenomena occurring in it.

To carry out the study, a laboratory membrane module was assembled and tested in an automated apparatus for gas separation measurements as functions of operative conditions and flow regimes. The results were analyzed on the basis of a mathematical model of the process in order to derive a full picture of the system behavior.

2. EXPERIMENTAL

Hollow fiber composite membranes manufactured by SNIA Fibre were utilized. The main characteristics of the membranes, indicated in Table 1, are described in more detail in Ref. *4*.

The membranes (about 100 fibers, 300 cm^2 active surfaces) were assembled in a stainless steel cylindrical module of 15 cm useful length and 1 cm internal diameter. The pressurized gas was fed at one end of the shell side of the module and discharged from the other end. The permeate stream flowed either cocurrently or countercurrently through the fibers lumen. The separation unit performances were measured for the CH_4/CO_2 system under various conditions by using the LIGASE apparatus described in Ref. *4*.

The experimental procedure consisted of feeding pure gases, or defined mixtures, to the module at a specified pressure, temperature, and flow rate. From the reading of the mass flowmeter (Matheson model 8240) and from gas chromatographic analysis of the gaseous currents (DANI model 3800), the attainment of steady state was determined, and its conditions were recorded.

TABLE 1
Main Characteristics of the Composite Hollow Fibers Utilized (*4*)

Type:	
Support polymer	Polysulfone
Coating	Aliphatic copolymer
Dimensions:	
External diameter (μm)	735 ± 9
Internal diameter (μm)	389 ± 12
Coating thickness (μm)	3.5 ± 1.5
Mechanical properties:	
Specific load (kg/mm^2)	1.14 ± 0.06
Extensibility (%)	42 ± 10
Young's modulus (kg/mm^2)	31 ± 1
Burst pressure (kg/cm^2)	36

3. RESULTS

The first set of data was obtained by testing the permeation characteristics for the individual gases CH_4 and CO_2 of the membranes utilized in the present work. In Table 2 the CO_2 and CH_4 permeability coefficients (K_{CO_2} and K_{CH_4}) and the separation factors ($\alpha CO_2/CH_4$) of the membranes are reported as functions of temperature and transmembrane pressure drop. While pressure seems to have a very small effect on permeation of the two single gases, temperature has a much larger effect both on permeability (K_{CO_2} and K_{CH_4} increase with increasing temperature) and selectivity. This trend indicates a higher permeation activation energy for CH_4 than for CO_2.

CO_2/CH_4 gas mixtures were utilized for studying the performances of the laboratory membrane separation unit as functions of operative conditions and flow regimes.

Effect of the "Stage Cut"

At constant temperature, pressure, and feed composition, the permeate composition (Y) is a function of the stage cut (θ, ratio of the permeate flow rate to the feed flow rate). This function specifically characterizes the flow

TABLE 2
Permeability Coefficients (K, st · cm^3/(min · cm^2 · atm) and Selectivities ($\alpha CO_2/CH_4$) of the Composite Hollow Fibers as Functions of Temperature and Transmembrane Pressure Drop (individual gas measurements)

Temperature (°C)	Transmembrane pressure drop (atm)								
	1			3			6		
	K_{CO_2}	K_{CH_4}	α	K_{CO_2}	K_{CH_4}	α	K_{CO_2}	K_{CH_4}	α
25	0.043	0.0118	3.63	0.043	0.0120	3.58	0.044	0.0127	3.47
45	0.066	0.0172	3.83	0.067	0.0178	3.76	0.068	0.0188	3.61
65	0.081	0.0269	3.01	0.082	0.0283	2.90	0.086	0.0307	2.80

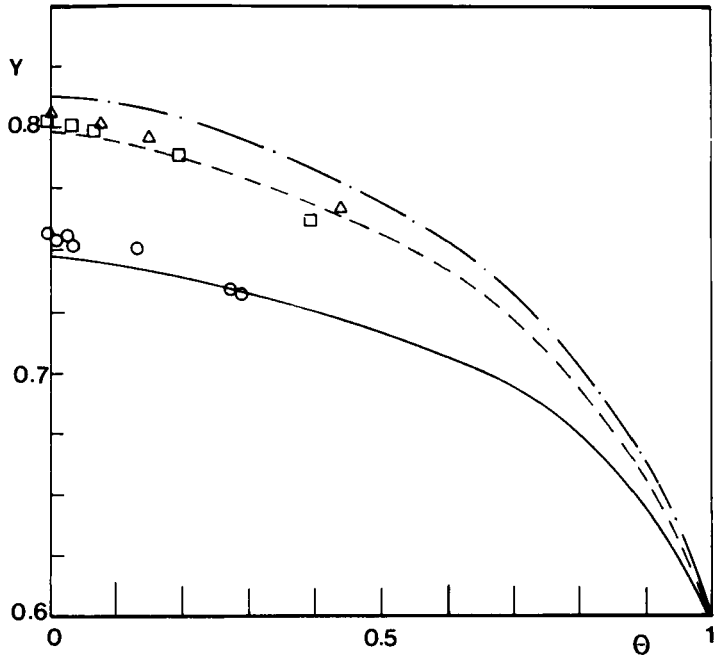

FIG. 1A. Experimental values (○, □, △ with $P_1 - P_2$ = 1, 3, 6 atm, respectively) and theoretical curves ——, — —, · · ·, obtained according to the Appendix with $P_1 - P_2$ = 1, 3, 6 atm, respectively) of CO_2 content in the permeate stream (Y) as a function of stage cut (θ) and the transmembrane pressure drop ($P_1 - P_2$). Inlet gas composition: 60% CO_2, 40% CH_4; temperature, 25°C.

regime into the module and the driving force distribution along the surface of the membrane.

In the present work a wide range of stage-cut values was adopted (0.005–0.8) by changing the feed flow rate with a constant membrane surface, and the effect on the CO_2 content was measured at temperatures between 25 and 65°C and transmembrane pressure drops between 1 and 6 atm for a 60% CO_2, 40% CH_4 gaseous mixture (Figs. 1A and 1B). All the curves obtained show asymptotic CO_2 content values (Y_a) when θ approaches 0. These values correspond to a situation of homogeneous composition of the gas streams on both the high and low pressure sides of the membrane. It follows that such values characterize the membrane properties rather than the module performances. Therefore, in the mathematical model (see Section 4), these Y_a values were taken into

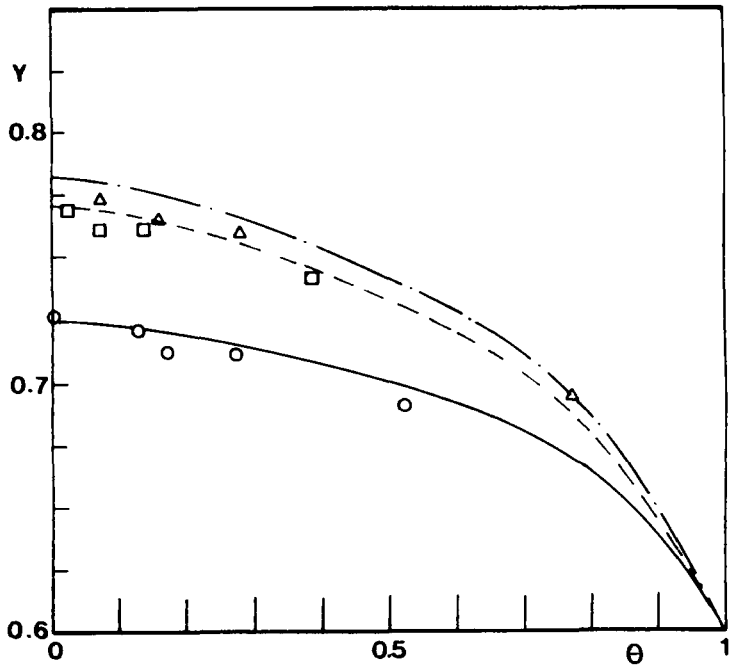

FIG. 1B. As in Fig. 1A, but at 65°C.

account to study the effect of temperature, pressure, and gas composition on the separation, while the whole function $Y = f(\theta)$ was used for characterizing the flow regime.

Effect of Temperature

Permeate flow rate and CO_2 content were measured at 25, 45, and 65°C at 1, 3, and 6 atm transmembrane pressure drop and at an asymptotic stage cut of 0.05 for a 60% CO_2, 40% CH_4 gaseous mixture (Fig. 2).

The increase in permeate flow rate and the decrease in the permeate CO_2 content with increasing temperature is in agreement with the characteristics of the membrane (Table 2: increase of CO_2 permeability and decrease in selectivity between 25 and 65°C).

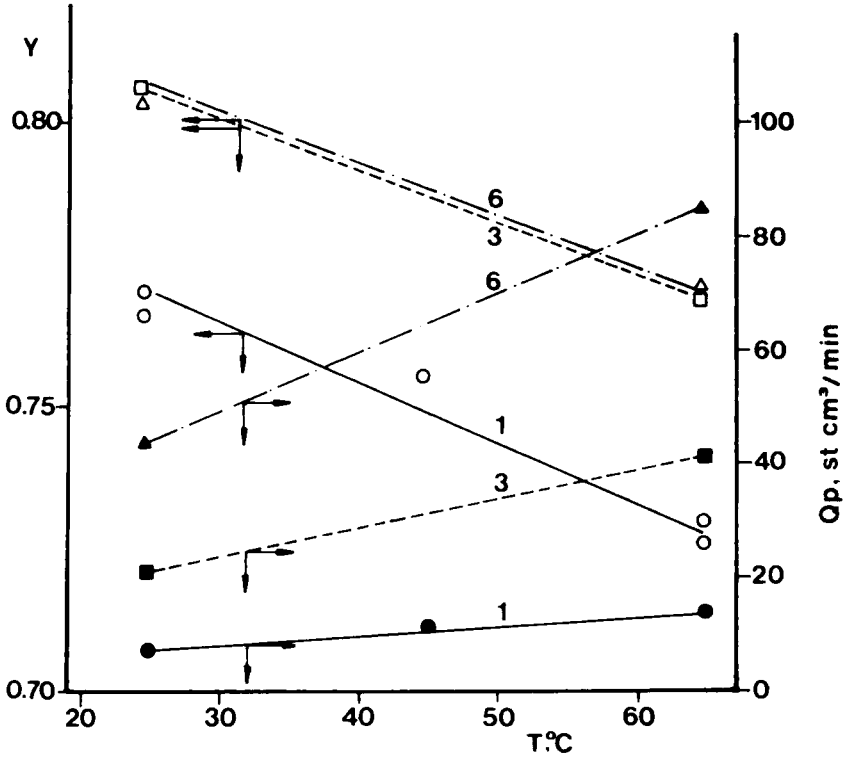

FIG. 2. CO_2 content (Y) and flow rate (Q_P) of the permeate stream as a function of temperature (T) and the transmembrane pressure drop ($P_1 - P_2$ = 1, 3, 6 atm). Inlet gas composition: 60% CO_2, 40% CH_4; stage cut $\approx$ 0.

Effect of Transmembrane Pressure Drop

In line with the mathematical model, the increase in transmembrane pressure drop ($P_1 - P_2$) is expected to increase both the flow rate and CO_2 content of the permreate. At ($P_1 - P_2$) values below 3 atm the experimental results were in agreement with the calculated ones. At higher pressures, both the experimental and the theoretical permeate flow rates increase, but the experimental CO_2 content remains practically constant while the calculated one increases (Figs. 1-3).

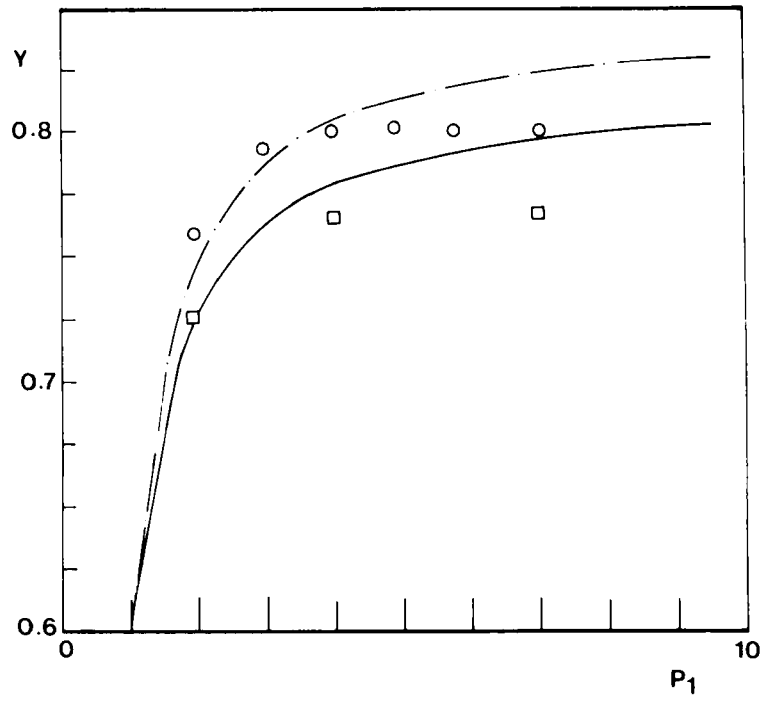

FIG. 3. Experimental values (O and □ at 25 and 65°C, respectively) and theoretical curves (- · - and —— obtained according to the Appendix at 25 and 65°C, respectively) of CO_2 content in the permeate stream (Y) as a function of pressure P_1 at one side of the membrane. The pressure on the other side of the membrane is P_2 = 1 ata; inlet gas composition: 60% CO_2, 40% CH_4; stage cut ≈ 0.

Effect of Mixture Composition

The asymptothic permeate CO_2 content (Y_a) was measured as a function of the feed CO_2 content (X) at various temperatures and pressures (Fig. 4). The improvement in the separation at lower temperatures and higher pressures is evident.

The relation $Y_a = f(X)$ is analogous to the equilibrium equation for distillation processes, and McCabe-Thiele diagrams could be constructed on this basis (*1*).

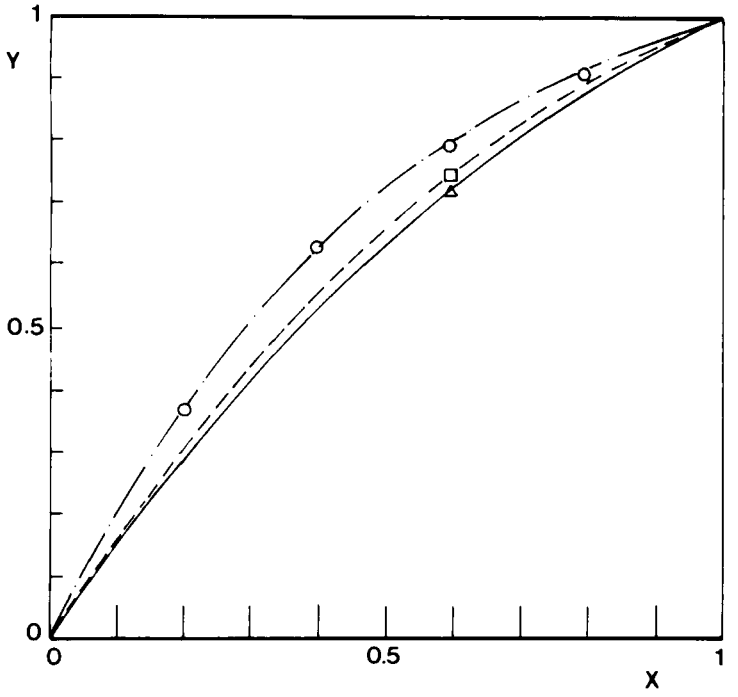

FIG. 4. Experimental values and theoretical curves (O, - · - at $P_1 - P_2 = 3$ atm and $T = 25°C$; □, - - at $P_1 - P_2 = 1$ atm and $T = 25°C$; △, —— at $P_1 - P_2 = 1$ atm and *T01 = 65°C) of* CO_2 content in the permeate stream (Y) as a function of CO_2 content in the feeding stream (X) with stage cut ≈ 0.

Effect of the Flow Pattern

A comparison of the performance when the system is operated cocurrently or countercurrently was derived from the results of permeate CO_2 content versus stage cut measured at 3 atm transmembrane pressure drop and at 28°C for a 60% CO_2, 40% CH_4 mixture (Fig. 5). For the two regimes, very small differences were obtained both for experimental and calculated values, particularly at low stage cuts.

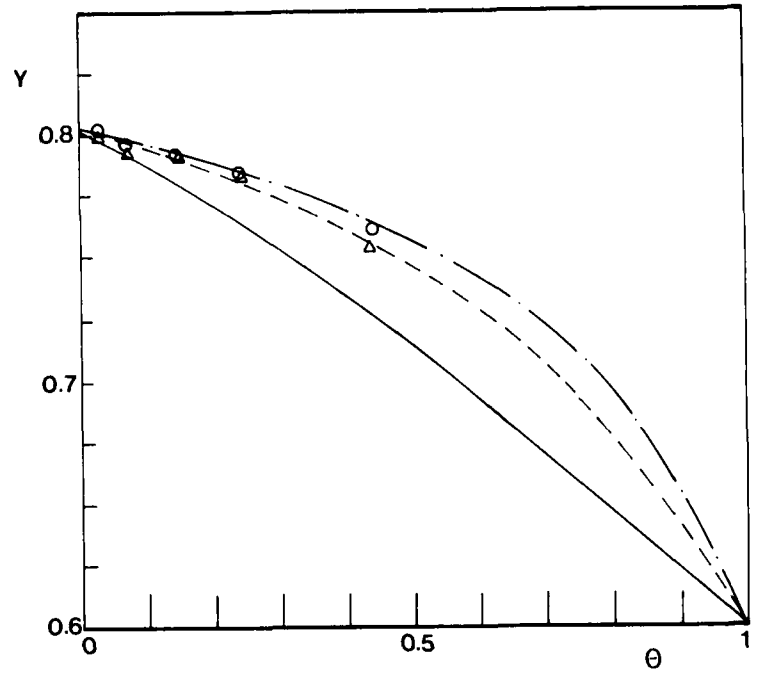

FIG. 5. Experimental values (O, Δ in countercurrent and cocurrent conditions, respectively) and theoretical curves (- · -, - -, —— obtained according to the Appendix for countercurrent, cocurrent, and perfect mixing conditions, respectively) of CO_2 content in the permeate stream (Y) as a function of stage cut (θ) and flow regime. Inlet gas composition: 60% CO_2, 40% CH_4; temperature, 28°C; transmembrane pressure drop, 3 atm.

4. MATHEMATICAL MODEL

Many mathematical models of the membrane gas separation process have been published (*5–8*). All of them are based on a simple theoretical picture of the mass transport phenomenon through the membrane, and incorporate, to various extents, the flow pattern effects on both the permeate and retentate sides of the membrane. The model considered in the present work is based on the same approach and on the hypothesis of an "ideal behavior" defined as follows:

Independent transport of the components of the mixture through the membrane

Linear relationship of the permeate flux to the difference of the partial pressure at the two sides of the membrane

Constant permeability and selectivity along the membrane

Negligible pressure drops both for the permeate and retentate gaseous streams

Theoretical "plug flow" cocurrent or countercurrent flow regimes, or perfect mixing conditions for each corresponding version of the model.

The solutions of the model for the three above-mentioned conditions are described in more detail in the Appendix. These solutions utilize a fourth order Runge-Kutta numerical integration of the differential equations of mass transport through the membrane. The integration starts from the section of the module where there is no convective contribution to the permeate stream (inlet section for cocurrent conditions, or outlet section of the pressurized gas for countercurrent conditions). In this section the composition of the permeate stream depends only on the membrane characteristics and the composition of the retentate stream X; it is equal to the asymptotic value mentioned above (Y_a) (*12*):

$$Y_a = \frac{D + \sqrt{D^2 + 4\alpha P_r(1 - \alpha)X}}{2(1 - \alpha)} \tag{1}$$

where

$$D = (1 - \alpha)(1 + XP_r) - P_r$$

When the inlet conditions and the characteristics of the membrane are known, integration of the model allows calculation of the outlet conditions as functions of the operative variables and the membrane area.

The predictions of the model are compared wtih experimental data in Figs. 1A, 1B, 3, 4, and 5.

In Fig. 5 the predicted behaviors of cocurrent, countercurrent, and perfectly mixed gas separation units are compared as functions of the module stage cut. The permeate CO_2 content is identical in all three cases when θ approaches 0, but when the stage cut increases, the highest CO_2 content is obtained in countercurrent conditions.

Also, the best recovery of the fast permeating component (CO_2) is obtained for the countercurrent case. The reason for this is the more

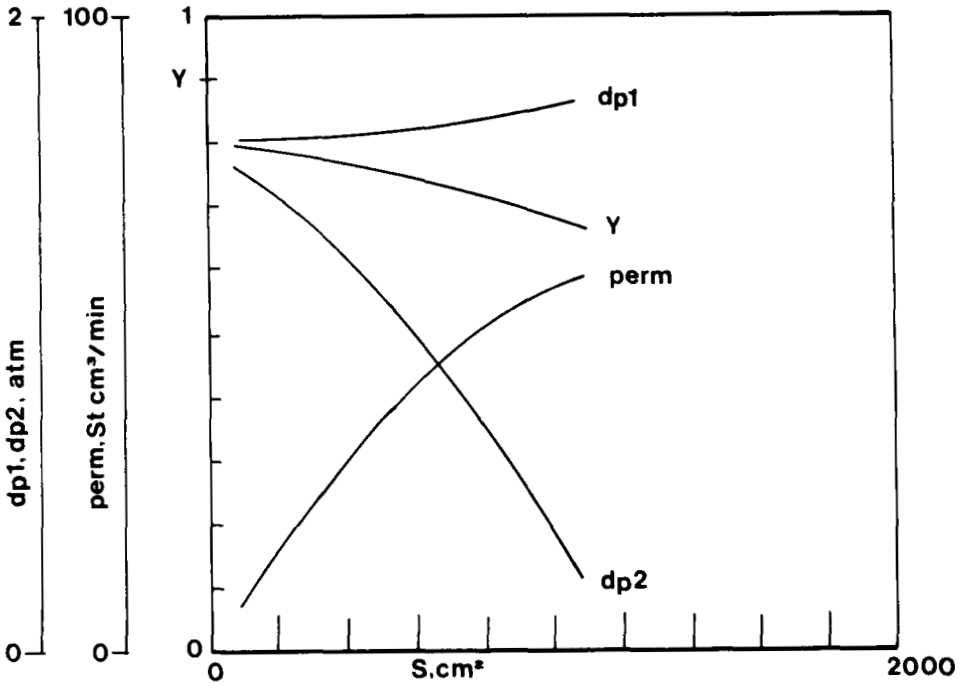

FIG. 6. Theoretical predictions of the driving force at the two ends of the module (dp_1, dp_2, CO_2 partial pressure, atm), CO_2 content in the permeate stream (Y), and CO_2 recovery in the permeate stream (perm) as a function of the membrane surface (S). Model parameters: $X_i = 0.6$; $K_{CO_2} = 0.08$ st · cm³/(cm² · min · atm); $\alpha = 3.5$; $P_1 = 4$ ata; $P_2 = 1$ ata; $Q_F = 100$ cm³/min. Countercurrent conditions.

efficient utilization of the driving force along the membrane surface: in Figs. 6–8 the driving force at the two ends of the module (differences, dp_1 and dp_2, of CO_2 partial pressure) is plotted versus the membrane surface for the three flow pattern conditions.

The lowest calculated permeate CO_2 content is obtained in the perfect mixing case ($dp_1 = dp_2$). Under cocurrent conditions the driving force at the inlet section remains constant, but it decreases very fast along the membrane, particularly for large surface modules. Under countercurrent conditions the driving force at the inlet section increases with the surface of the membrane (the permeate stream is diluted), while at the outlet section it decreases. The average value of the driving force under

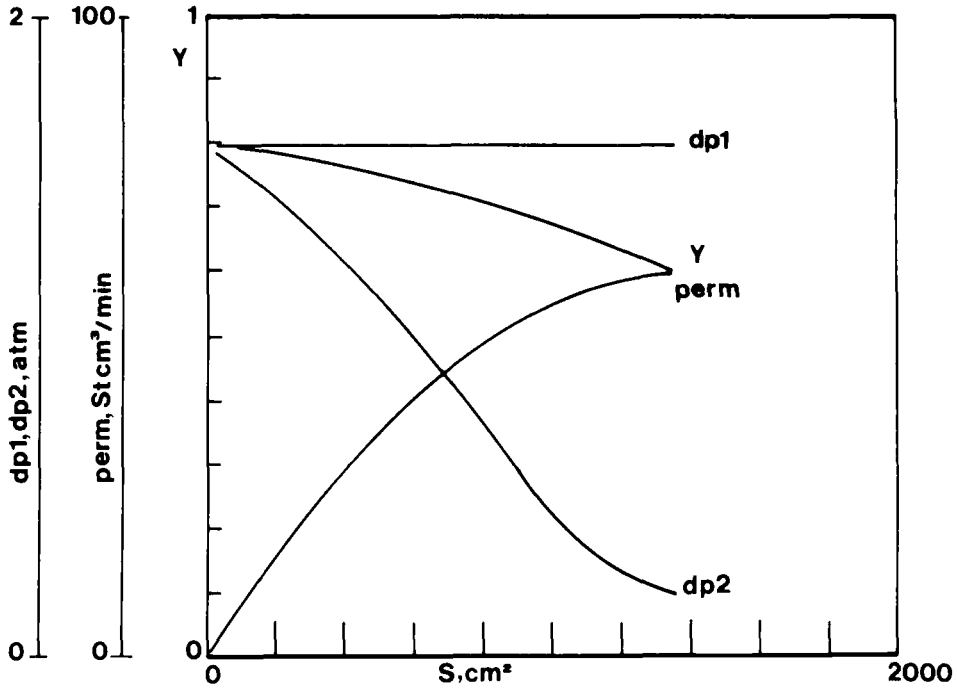

FIG. 7. As in Fig. 6, but under cocurrent conditions.

countercurrent conditions is higher than under cocurrent conditions, but the difference between these two situations is quite small in terms of both recovery and permeate CO_2 content (Figs. 5–8).

5. DISCUSSION

The mathematical model used in the present work is based on the hypothesis of "ideal behavior" of the system, although nonideal effects are not uncommon in this field. This is due to:

(a) Competition of the gaseous mixture components in the permeation process (*9*), and the consequent differences between the

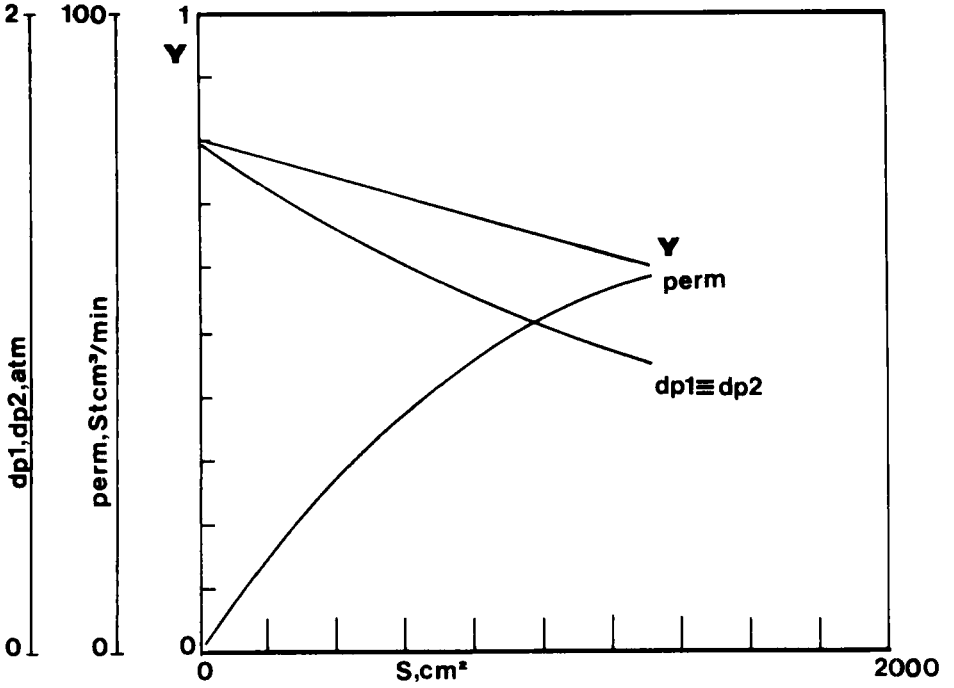

FIG. 8. As in Fig. 6, but under perfect mixing conditions.

observed selectivity and permeation rate for mixed gas, and the corresponding values derived from pure component data (*8*).

(b) Structural changes of the hollow fibers under pressurization, and the consequent effect on permeation rate and selectivity (*10*). In addition, enhancement of membrane defects can occur at high pressure and temperature.

(c) Cooling effects due to expansion of the permeate gas, and the consequent possible condensation, in some cases, of components of the mixture (*8*).

(d) Permeate pressure build-up inside the narrow fiber, and the consequent reduction of the transport driving force (*11*). The pressure drop of the retentate stream also contributes to the driving force reduction along the membrane surface.

(e) Nonideal flow regimes (stagnation points, obstructions, etc.), and the consequent difference between the degree of removal of the

fast permeating species for portions of gas having different residence times into the permeator (*12*). Therefore, the module performance is never perfectly described by plug flow or perfect mixing models, although a good module design can make the system approach plug flow conditions that are more appropriate for an efficient separation.

In the present work such "nonideal" effects seem not to be severe because the model fits the experimental data very well in most cases. A significant departure from the model predictions occurs only at high pressure ($P_1 > 4$ ata), probably as a consequence of Point b above.

6. CONCLUSIONS

The performances of the membrane separation unit were measured for CH_4/CO_2 mixtures as functions of a number of operative variables. The extent of separation was considerably affected by these variables, thus indicating possible ways for process optimization. To this end, a mathematical model of the process represents a powerful tool to predict the behavior of the system in a broad range of conditions and to define effective optimal situations.

Simple mathematical models, such as the one adopted in the present work, are useful, but the accuracy of the mathematical predictions should be high enough to allow reliable conclusions. The experimental results of the present work indicate that the departure from "ideal conditions" adopted for the mathematical simulation of the process is negligible in most cases.

APPENDIX: MATHEMATICAL MODEL OF THE MEMBRANE GAS SEPARATION PROCESS, TWO COMPONENTS SYSTEM, AND "IDEAL CONDITIONS" (see Section 4 and Symbols)

The approach utilized to calculate the theoretical values of Figs. 1 and 3–8 is basically the same as in classical papers describing modeling of membrane separation processes (*5–8*).

A.1. Perfect Mixing Conditions

In this situation the gas composition at both sides of the membrane is homogeneous in the permeator and equal to the exit gas composition (Fig. 9a). The solution for the unknown parameters (Y_o, X_o, S) becomes very simple because the following equations hold:

Mass balance equation:

$$X_i = (1 - \theta)X_o + \theta Y_o \tag{A.1.1}$$

Mass transport equation:

$$Y_o = F(X_o) \tag{A.1.2}$$

where the function F is indicated in Eq. (1).

Surface required:

$$S = \frac{Q_F \theta Y_o}{K_{CO_2}(P_1 X_o - P_2 Y_o)} \tag{A.1.3}$$

A.2. Cocurrent Conditions

In this situation the gas composition of both the permeate and retentate streams changes along the permeator due to transport through the membrane (Fig. 9b). The unknown functions $Y = f(S)$ and $X = f'(S)$ can be derived from the integration of mass balance equations for a differential area element dS:

$$-d(qX) = dSK_{CO_2}(P_1 X - P_2 Y) \tag{A.2.1}$$

$$-d(qX) = d(hY) \tag{A.2.2}$$

$$dq = dh \tag{A.2.3}$$

These equations can be integrated by introducing an adimensional parameter $q'' = q/Q_F$ and by considering an equation of mass balance

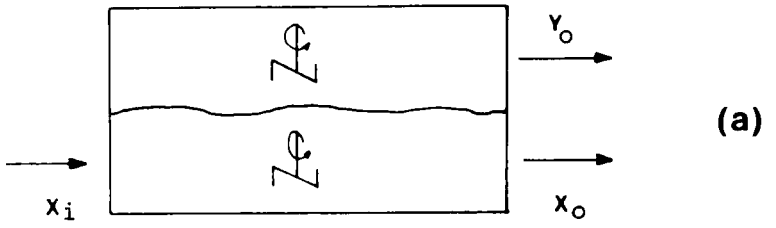

PERFECT MIXING CONDITIONS

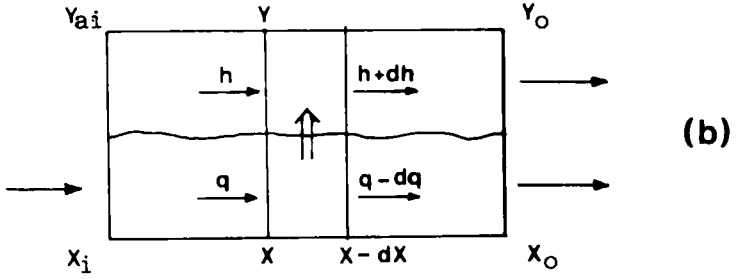

COCURRENT PLUG FLOW CONDITIONS

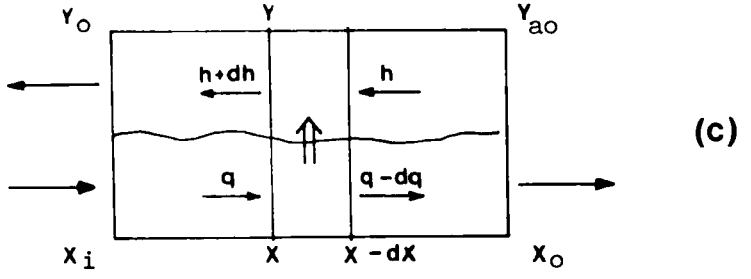

COUNTERCURRENT PLUG FLOW CONDITIONS

FIG. 9. Theoretical model schemes.

between the inlet section and the current one:

$$\frac{dq''}{dX} = \frac{q''}{X + \dfrac{\alpha}{(1-\alpha) + (P_r - 1)/(X - P_r Y)}} \tag{A.2.4}$$

$$Y = \frac{X_i - Xq'}{1 - q''} \qquad \text{for } X < X_i \tag{A.2.5}$$

These equations are integrated by numerical methods for the inlet section where the values of the variables are known:

$$X = X_i; \qquad Y = F(X_i); \qquad q'' = 1 \tag{A.2.6}$$

until the exit conditions are found:

$$X = X_o; \qquad Y_o = \frac{X_i - (1-\theta)X_o}{\theta}; \qquad q'' = 1 - \theta \tag{A.2.7}$$

The surface required is obtained by integrating the mass transport equation:

$$S = \frac{Q_F}{P_1 K_{CO_2}} \int_{1-\theta}^{1} \frac{dq''}{(X - P_r Y) + [(1-X)P_r(1-Y)]/\alpha} \tag{A.2.8}$$

A.3. Countercurrent Conditions

As in cocurrent conditions, the gas composition changes along the permeator and analogous differential equations can be used (Fig. 9c).

If the adimensional parameter $q' = q/(Q_F(1-\theta))$ is introduced, the equations to be solved are

$$\frac{dq'}{dx} = \frac{q'}{X + \dfrac{\alpha}{(1-\alpha) + (P_r - 1))/(X - P_r Y)}} \tag{A.3.1}$$

$$Y = \frac{X_{q'} - X_o}{q' - 1}, \qquad \text{for } X > X_o \tag{A.3.2}$$

These equations are integrated from the outlet section where

$$X = X_o; \qquad Y = F(X_o); \qquad q' = 1 \tag{A.3.3}$$

until the inlet conditions are found:

$$X = X_i; \qquad Y_i = \frac{X_i - (1 - \theta)X_o}{\theta}; \qquad q' = \frac{1}{1 - \theta} \tag{A.3.4}$$

The surface required is obtained by integrating the mass transport equation:

$$S = \frac{Q_F}{P_1 K_{CO_2}} \int_{1/(1-\theta)}^{1} \frac{dq'}{(X - P_r Y) + [(1 - X) - P_r(1 - Y)]/\alpha} \tag{A.3.5}$$

SYMBOLS

Y	concentration of the faster permeating component (CO_2) in the permeate stream ($CO_2/(CO_2 + CH_4)$ molar ratio)
X	concentration of CO_2 in the retentate stream ($CO_2/(CO_2 + CH_4)$ molar ratio)
K_{CO_2}, K_{CH_4}	permeability coefficient through the membrane ($st \cdot cm^3/(min \cdot cm^2 \cdot atm)$) of the components CO_2 and CH_4, respectively
α	$= K_{CO_2}/K_{CH_4}$, membrane selectivity factor
P_1, P_2	pressure (ata) on the membrane high (1) and low (2) pressure sides, respectively
P_r	$= P_1/P_2$, pressure ratio
dp_1, dp_2	difference of CO_2 partial pressure at the two ends of the module (atm)
S	membrane surface (cm^2)
Q_F, Q_P, q, h	gaseous flow rates ($st \cdot cm^3/min$): feed inlet, permeate outlet, high pressure side, low pressure side, respectively
θ	$= Q_P/Q_F$, stage cut of the permeator
perm	$= Q_P Y$, CO_2 recovery in the permeate stream

Subscripts

a	asymptotic conditions
i, o	feed stream inlet and outlet sections, respectively

REFERENCES

1. S. A. Stern, "The Separation of Gases by Selective Permeation," in *Membrane Separation Processes* (P. Meares, ed.), Elsevier, Amsterdam, 1976, pp. 295–326.
2. S. L. Matson, J. Lopez, and J. A. Quinn, *Chem. Eng. Sci., 38*(4), 503 (1983).
3. W. J. Schell, *Hydrocarbon Process.,* (8), 43 (1983).
4. C. Fabiani, M. Pizzichini, L. Bimbi, L. Visentini, G. Quaglia, and A. Ciaperoni, *Sep. Sci. Technol., 21,* 1111 (1986).
5. S. A. Stern and S. C. Wang, *J. Membr. Sci., 4,* 141 (1978).
6. W. P. Walawender and S. A. Stern, *Sep. Sci. Technol., 7,* 553 (1972).
7. C. T. Blaisdell and K. Kammermeyer, *Chem. Eng. Sci., 28,* 1249 (1973).
8. J. E. Hogsett and W. H. Mazur, *Hydrocarbon Process.,* (8), 52 (1983).
9. R. T. Chern, W. J. Koros, E. S. Sanders, and R. Yui, *J. Membr. Sci., 15,* 157 (1983).
10. S. A. Stern, F. J. Onorato, and C. Libove, *AIChE J., 23,* 567 (1977).
11. C. Y. Pan and H. W. Habgood, *Can. J. Chem. Eng., 56,* 210 (1978).
12. D. L. MacLean, D. J. Stookey, and T. R. Metzeger, *Hydrocarbon Process.,* (8), 47 (1983).

Received by editor November 22, 1988